

Shifting the ISAC Trade-Off with Fluid Antenna Systems

Jiaqi Zou, *Graduate Student Member, IEEE*, Hao Xu, *Member, IEEE*, Chao Wang, *Senior Member, IEEE*, Lvxin Xu, Songlin Sun, *Senior Member, IEEE*, Kaitao Meng, *Member, IEEE*, Christos Masouros, *Fellow, IEEE*, and Kai-Kit Wong, *Fellow, IEEE*

Abstract—As an emerging reconfigurable antenna technology, fluid antenna system (FAS) has the capability of improving both sensing and communication (S&C) performance by switching the antenna position over the available ports. This increased spatial degree-of-freedom (DoF) by FAS can be translated into enlarging the trade-off region for integrated sensing and communication (ISAC). In this letter, we propose a signal model for FAS-enabled ISAC and jointly optimize the transmit beamforming and port selection of FAS. In particular, our objective is to minimize the transmit power, while satisfying both communication and sensing requirements. To tackle this, an efficient iterative algorithm based on sparse optimization, convex approximation, and a penalty approach is developed. Our simulation results illustrate that the proposed scheme can attain 33% reductions in the transmit power with guaranteed S&C performance, showing the great potential of FAS for striking a balance between S&C in ISAC systems.

Index Terms—Fluid antenna system, ISAC, port selection.

I. INTRODUCTION

REGARDED widely as one of the emerging technologies in next-generation wireless communications, integrated sensing and communications (ISAC) offers an attractive way of supporting these two previously separate functionalities [1]. Various design methodologies have been proposed to unlock the potential of ISAC with shared signal processing techniques and even hardware devices. A unique feature of ISAC is to meet both sensing and communications (S&C) requirements and balance the conflicting S&C objectives. For instance, the fundamental trade-offs between the communication sum-rate and Cramér-Rao bound (CRB) for target parameter estimation were studied in [2]. A novel performance metric was recently proposed in [3] to measure the sensing-centric energy efficiency, and the trade-off between communication-centric and sensing-centric energy efficiency was also investigated.

The unveiled potential of ISAC is also attributed to the development of multiple-input multiple-output (MIMO) due to its multiplexing and diversity gain. Currently, as an emerging antenna technology, fluid antenna system (FAS) exploits more favorable channel conditions and spatial diversity incorporating shape and position flexibility in reconfigurable antennas

[4], [5], [6]. FAS introduces additional degrees of freedom (DoFs) in the physical layer that was not possible before.

Despite the growing attention for FAS in the area of antenna design, the use of FAS in enhancing wireless communication performance has not been considered until the work of [7]. More recently, the work in [8] utilized a switchable antenna port and proposed a novel fast fluid antenna multiple access (FAMA) scheme to avoid inter-user interference. To prevent fast port switching on a symbol-by-symbol basis and reduce the complexity, slow FANA was later proposed in [9]. In [10], the two-user slow FAMA system was studied and the outage performance was investigated under a fully correlated channel model. Channel estimation for FAS is an important problem and was studied in [11]. To further reduce the overhead for channel state information (CSI) estimation of all the ports, [12] adopted a deep learning approach. Moreover, [13] proposed a bandit-learning-based framework for online port selection, eliminating the requirements of instantaneous full CSI.

Although FAS has demonstrated great communication performance, its merit to support ISAC, especially for the sensing functionality, has not been well investigated. Compared with the conventional fixed antenna selection for ISAC [14], FAS allows for optimizing the antenna positions (i.e., ports) within a constrained space, yielding increased DoFs for enhancing the integration gain in ISAC systems, e.g., choosing an antenna position with higher channel correlation between sensing and communication [15]. In this letter, we investigate FAS-enabled ISAC, where we consider a FAS base station (BS) that simultaneously achieves multicast communication and target sensing. It is worth pointing out that most recently, [16] investigated the FAS design at the BS to maximize the sum rate of communication users (CUs) under a sensing constraint using deep reinforcement learning. But the instantaneous communication and the trade-off between S&C is not well understood.

In this letter, we aim to minimize the transmit power, considering the signal-to-noise ratio (SNR) requirement for sensing, the SNR requirement for communication, and the constraint of available ports. Our aim is to explore the enhancements in the ISAC trade-off that the FAS capability offers. Whereas the considered problem is NP-hard, we propose an iterative optimization algorithm leveraging sparse optimization and linear matrix inequality to transform the nonconvex problem into a sequence of convex optimization problems. Simulation results reveal that the proposed method for the FAS-assisted ISAC system leads to a significant reduction in power consumption and demonstrates the great potential advantage for improving the flexibility of balancing the S&C performance.

J. Zou is with the Department of Electronic Engineering, Tsinghua University, Beijing 100084, China. (e-mail: jqzou@mail.tsinghua.edu.cn).

L. Xu, and S. Sun are with the School of Information and Communication Engineering, Beijing University of Posts and Telecommunications, Beijing 100876, China. (E-mail: {xulvxin, slsun}@bupt.edu.cn).

H. Xu, K. Meng, C. Masouros, and K. K. Wong are with the Department of Electronic and Electrical Engineering, University College London, London, UK. (E-mail: {hao.xu, kaitao.meng, c.masouros, kai-kit.wong}@ucl.ac.uk). K. K. Wong is also affiliated with the Department of Electronic Engineering, Kyung Hee University, Yongin-si, Gyeonggi-do 17104, Korea. The work of H. Xu is supported in part by the Engineering and Physical Sciences Research Council (EPSRC) under grant EP/W026813/1, and the National Nature Science Foundation of China 62061017.

C. Wang is with Integrated Service Networks Lab, Xidian University, Xi'an 710071, China. (E-mail: drchao wang@126.com).

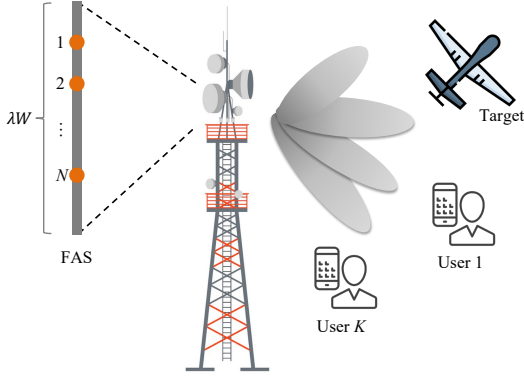


Fig. 1. System model.

II. SYSTEM MODEL

A. System Setting

As shown in Fig. 1, we consider a system with a multicast ISAC BS and K mobile CUs. The BS transmits a common signal to the users and utilizes the echo signals to perform potential target sensing. Each mobile user has a fixed-position antenna. Differently, the BS is equipped with an N -antenna FAS, where M predetermined ports are uniformly distributed along a linear space of length λW , in which λ is the carrier wavelength and W is the normalized size of FAS. The N antennas can change their positions among the M available ports such that the ISAC performance can be enhanced. Compared with the traditional MIMO, the port switching capability of FAS gives more spatial DoF to the ISAC BS.

B. Multicast Communication Performance

Let $s \sim \mathcal{CN}(0, 1)$ denote the communication signal to be transmitted. The received signal at the k th user is given by

$$y_k = \mathbf{h}_k^H \mathbf{w} s + n_k, \quad (1)$$

where $\mathbf{h}_k \in \mathbb{C}^{M \times 1}$, $\mathbf{w} \in \mathbb{C}^{M \times 1}$, and $n_k \sim \mathcal{CN}(0, \sigma_c^2)$ denote the channel from the BS to the k th user, the ISAC beamforming vector, and the additive white Gaussian noise (AWGN) received at the k th user, respectively. It is also assumed that only N out of M ports are activated to generate the ISAC waveform at the BS. Thus $\|\mathbf{w}\|_0 = N$, where $\|\cdot\|_0$ represents the L_0 norm. For the communication channel, we follow [17] to express the spatial correlation among the ports as \mathbf{J} . Decomposing \mathbf{J} , we have $\mathbf{J} = \mathbf{U}_{\text{tx}} \mathbf{\Lambda}_{\text{tx}}^H \mathbf{U}_{\text{tx}}$, where $\mathbf{\Lambda}_{\text{tx}} \in \mathbb{C}^{M \times M}$ is a diagonal matrix whose elements are the eigenvalues of the spatial correlation matrix \mathbf{J} and the columns of $\mathbf{U}_{\text{tx}} \in \mathbb{C}^{M \times M}$ are the corresponding eigenvectors. Then, the spatially correlated channel can be given as

$$\mathbf{h}_k = \mathbf{g}^H \sqrt{\mathbf{\Lambda}_{\text{tx}}^H} \mathbf{U}_{\text{tx}}^H, \quad (2)$$

where $\mathbf{g} \sim \mathcal{CN}(\mathbf{0}, \mathbf{I}_M)$. Accordingly, the communication SNR at the k th user is given by

$$\gamma_{c,k} = \frac{|\mathbf{h}_k^H \mathbf{w}|^2}{\sigma_c^2}. \quad (3)$$

C. Target Sensing Performance

Regarding sensing, we consider a colocated monostatic MIMO radar system equipped with N_r receive antennas. Then the echo signal received at the sensing receiver is given by

$$\mathbf{y}_r = \mathbf{A}(v) \mathbf{w} s + \mathbf{z}_r, \quad (4)$$

in which $\mathbf{A}(v) = \beta \boldsymbol{\alpha}_r(v_r) \boldsymbol{\alpha}_t^T(v_t)$ and $\mathbf{z}_r \sim \mathcal{CN}(\mathbf{0}, \sigma_r^2 \mathbf{I}_{N_r})$ denote the target response matrix and the AWGN, respectively. Additionally, β represents the reflection coefficient, $\boldsymbol{\alpha}_t(v_t) = [1, \dots, e^{-j2\pi(N_t-1)\Delta_t \sin(v_r)}]$ and $\boldsymbol{\alpha}_r(v_r) = [1, \dots, e^{-j2\pi(N_r-1)\Delta_r \sin(v_r)}]$ denote the transmitting and receiving steering vectors, respectively, where Δ_t and Δ_r are the antenna spacing of transmit and receive antennas, respectively. Here, we consider the straightforward scenario of single-target sensing for the initial exploration of FAS-ISAC. However, our proposed method can be extended to multiple-target sensing by incorporating reflections from multiple targets. As we consider the monostatic colocated MIMO radar, we have the identical angle of departure (AOD) and angle of arrival (AOA) of the target as in existing literature [3], [2], denoted as $v_t = v_r = v$.

It is worth noting that we adopt the fixed antenna array at the sensing receiver for angle estimation. Accordingly, the average sensing SNR is formulated as

$$\gamma_r = \frac{\|\mathbf{A}(v) \mathbf{w}\|_2^2}{\sigma_r^2}. \quad (5)$$

III. JOINT PORT SELECTION AND DUAL-FUNCTIONAL BEAMFORMING OPTIMIZATION

Based on the above models, we now turn our attention to designing a joint port selection and beamforming scheme for FAS-enabled ISAC. Our objective is to minimize the total transmit power under the constraints of the minimum sensing SNR requirement r_s , the minimum communication SNR requirement r_c , and the number of activated ports. The considered problem can be formulated as

$$\underset{\mathbf{w}}{\text{minimize}} \|\mathbf{w}\|_2^2 \quad (6a)$$

$$\text{s.t. } \gamma_r \geq r_s, \gamma_{c,k} \geq r_c, k \in \mathcal{K}, \|\mathbf{w}\|_0 = N, \quad (6b)$$

where $\mathcal{K} = \{1, \dots, K\}$ denotes the CU set. Different from traditional multicast ISAC systems, the additional sparse constraint enforces that only $N < M$ antenna ports are activated to generate the ISAC signal.

Problem (6) is challenging to handle, since the constraints in (6b) are all nonconvex. Besides, the port selection problem is a nonconvex combinatorial optimization problem due to the sparse constraint in (6b), which makes problem (6) more challenging to handle. To deal with the problem (6), we adopt sparse optimization to propose an iterative optimization algorithm [19]. Firstly, we adopt a penalty method to move the nonconvex sparse constraint into the objective function and obtain the following penalized problem:

$$\underset{\mathbf{w}}{\text{minimize}} \|\mathbf{w}\|_2^2 + \lambda \|\mathbf{w}\|_0 \quad (7a)$$

$$\text{s.t. } \gamma_r \geq r_s, \gamma_{c,k} \geq r_c, k \in \mathcal{K}, \quad (7b)$$

where λ is a penalized parameter that can balance between the objective of minimizing the number of the selected ports

and that of minimizing the total power. Thus, we can adjust λ to select N ports. However, $\|\mathbf{w}\|_0$ is still nonconvex, which makes the objective function difficult to handle. Considering that the L_1 norm, $\|\mathbf{w}\|_1$, serves as a convex approximation of $\|\mathbf{w}\|_0$, we resort to the convex approximation of (7) for obtaining its local optimal solution, i.e.,

$$\underset{\mathbf{w}}{\text{minimize}} \|\mathbf{w}\|_2^2 + \lambda \|\mathbf{w}\|_1 \quad \text{s.t. (7b).} \quad (8)$$

For each λ , we can find $\hat{\lambda}$ to reformulate problem (8) as

$$\underset{\mathbf{w}}{\text{minimize}} \|\mathbf{w}\|_2^2 + \hat{\lambda} \|\mathbf{w}\|_1 \quad \text{s.t. (7b).} \quad (9)$$

Since the objective function of problem (9) is a convex approximation of that of problem (7), we can solve problem (9) iteratively to obtain a local optimal solution of problem (7) [20]. However, the constraints in problem (9) are still nonconvex, making the problem nontractable. To reformulate problem (9) as a tractable one, we introduce an auxiliary matrix $\mathbf{X} = \mathbf{w}\mathbf{w}^H$ to reformulate problem (9) as

$$\underset{\mathbf{X}}{\text{minimize}} \text{Tr}(\mathbf{X}) + \hat{\lambda} \text{Tr}(\mathbf{1}_{N \times N} |\mathbf{X}|) \quad (10a)$$

$$\text{s.t. } \frac{\text{Tr}(\mathbf{h}_k^H \mathbf{X} \mathbf{h}_k)}{\sigma_c^2} \geq r_c, \quad \frac{\text{Tr}(\mathbf{A}(v) \mathbf{X} \mathbf{A}^H(v))}{\sigma_r^2} \geq r_s, \quad (10b)$$

$$\text{rank}(\mathbf{X}) = 1, \quad (10c)$$

where the reformulation of the objective function is due to the fact that $\|\mathbf{w}\|_1^2 = \mathbf{1}_{N \times 1}^T |\mathbf{X}| \mathbf{1}_{N \times 1} = \text{Tr}(\mathbf{1}_{N \times N} |\mathbf{X}|)$. We observe that problem (10) is still nonconvex because of the rank-1 constraint (10c). To tackle this problem, we exploit [3, Lemma 1] and reformulate problem (10) as

$$\underset{\mathbf{X}, \mathbf{w}}{\text{minimize}} \text{Tr}(\mathbf{X}) + \hat{\lambda} \text{Tr}(\mathbf{1}_{N \times N} |\mathbf{X}|) \quad (11a)$$

$$\text{s.t. } \begin{bmatrix} \mathbf{X}, & \mathbf{w} \\ \mathbf{w}^H, & \mathbf{1} \end{bmatrix} \succeq \mathbf{0}, \quad \text{Tr}(\mathbf{X}) \leq \mathbf{w}^H \mathbf{w}, \quad (11b)$$

$$(10b). \quad (11c)$$

Although problem (11c) is still nonconvex, we can further adopt successive convex approximation (SCA) to approximate it as a sequence of convex problems, given by

$$\underset{\mathbf{X}, \mathbf{w}}{\text{minimize}} \text{Tr}(\mathbf{X}) + \hat{\lambda} \text{Tr}(\mathbf{1}_{N \times N} |\mathbf{X}|) \quad (12a)$$

$$\text{s.t. } \begin{bmatrix} \mathbf{X}, & \mathbf{w} \\ \mathbf{w}^H, & \mathbf{1} \end{bmatrix} \succeq \mathbf{0}, \quad \text{Tr}(\mathbf{X}) \leq -\mathbf{w}_{l-1}^H \mathbf{w}_{l-1} + 2\text{Re}(\mathbf{w}_{l-1}^H \mathbf{w}), \quad (12b)$$

$$(10b). \quad (12c)$$

Therefore, we can adopt bisection search over $\hat{\lambda}$ to solve a sequence of problems (12) for getting a local optimal solution to problem (6). To further increase the sparsity of \mathbf{w} , we adopt the iteratively re-weighted l_1 -norm penalty in [21]. For completeness, we sketch the iteratively re-weighted l_1 -norm penalty approach. In particular, by introducing an auxiliary matrix \mathbf{U} , we construct a new penalty problem as

$$\underset{\mathbf{X}, \mathbf{w}}{\text{minimize}} \text{Tr}(\mathbf{X}) + \hat{\lambda} \text{Tr}(\mathbf{U} |\mathbf{X}|) \quad (13a)$$

$$\text{s.t. (12b), (10b)}. \quad (13b)$$

The iterative algorithm is given in Algorithm 1. After obtaining

Algorithm 1 Iteratively Re-Weighted l_1 -Norm Penalty Approach.

- 1: Set $j = 0$ and initialize $\mathbf{U}^{(j)} = \mathbf{1}_{N \times N}$;
- 2: **while** 1 **do**
- 3: **while** not converged **do**
- 4: Solve the following weighted l_1 -norm problem to obtain \mathbf{X}^* and \mathbf{w}^*

$$\underset{\mathbf{X}, \mathbf{w}}{\text{minimize}} \text{Tr}(\mathbf{X}) + \hat{\lambda} \text{Tr}(\mathbf{U}^{(j)} |\mathbf{X}|), \quad \text{s.t. (13b)}$$
- 5: Update $\mathbf{w}_{l-1} = \mathbf{w}^*$
- 6: **end while**
- 7: Output \mathbf{X}^*
- 8: Update the weight matrix $\mathbf{U}^{j+1}(m, n) = 1/(|\mathbf{X}^*(m, n)| + \epsilon)$ for each $m, n = 1, \dots, M$
- 9: $j = j + 1$, if j exceeds the threshold, output \mathbf{U}^* , break.
- 10: **end while**

Algorithm 2 Proposed Joint Port Selection and ISAC Beamforming Optimization.

- 1: Initialize $\hat{\lambda}_L$ and $\hat{\lambda}_U$. Set the tolerance $\epsilon \ll 1$ and $\hat{\lambda} = \frac{\lambda_U + \lambda_L}{2}$
- 2: **while** $\hat{\lambda}_U - \hat{\lambda}_L > \epsilon$ **do**
- 3: **while** not converged **do**
- 4: Solve the following weighted l_1 -norm problem to obtain \mathbf{X}^* and \mathbf{w}^*

$$\underset{\mathbf{X}, \mathbf{w}}{\text{minimize}} \text{Tr}(\mathbf{X}) + \hat{\lambda} \text{Tr}(\mathbf{U}^{(*)} |\mathbf{X}|), \quad \text{s.t. (13b)}$$
- 5: Update $\mathbf{w}_{l-1} = \mathbf{w}^*$
- 6: **end while**
- 7: If $\|\mathbf{w}\|_0 > N$, set $\hat{\lambda}_L = \hat{\lambda}$, else set $\hat{\lambda}_U = \hat{\lambda}$.
- 8: **end while**

\mathbf{U}^* , we adopt bisection search algorithm to find λ for making $\|\mathbf{w}\|_0 = N$, which is given by Algorithm 2.

IV. SIMULATION RESULTS

Here, we provide the simulation results of the proposed joint beamforming and port selection algorithm for FAS-enabled ISAC. Unless stated otherwise, we have set $M = 32$ with $W = 2$ in the simulations. Compared to conventional uniformly-distributed antenna systems, which are limited to only four antennas with half-wavelength spacing within the restricted space of 2λ , FAS permits the implementation of a larger number of active antennas and flexible positioning among the ports. Besides, we assume that $\sigma_c^2 = \sigma_r^2 = 1$, and $K = 10$. For sensing, we consider a point-like target located at $v_t = v_r = v = 60^\circ$ with the reflection coefficient $\beta = 0.1$.

We first examine the convergence performance of our proposed algorithm, as shown in Fig. 2. In the initial iterations, due to the small value of $\hat{\lambda}$, the sparsity of \mathbf{w} is relatively low. Consequently, the number of selected transmit antennas exceeds the constraint, resulting in lower transmit power. As the iterations progress, the sparsity of \mathbf{w} gradually improves,

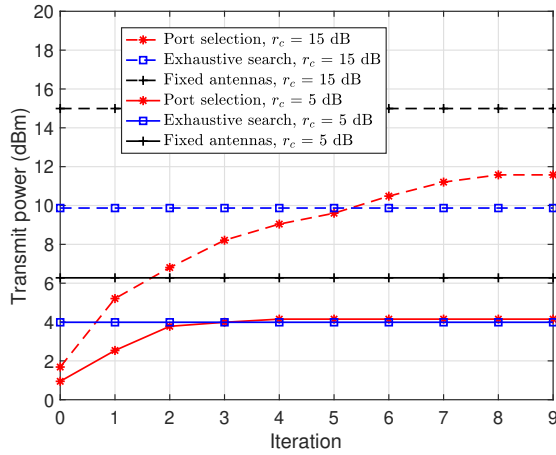


Fig. 2. Transmit power versus iteration number, compared with the baseline and the optimal solution, with $N = 4$, $r_s = 5$ dB.

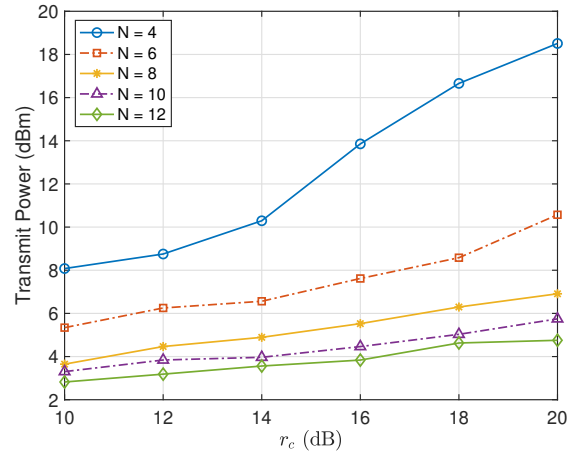


Fig. 4. Transmit power versus different communication SNR thresholds r_c , under different number of selected ports N , with $r_s = 5$ dB.

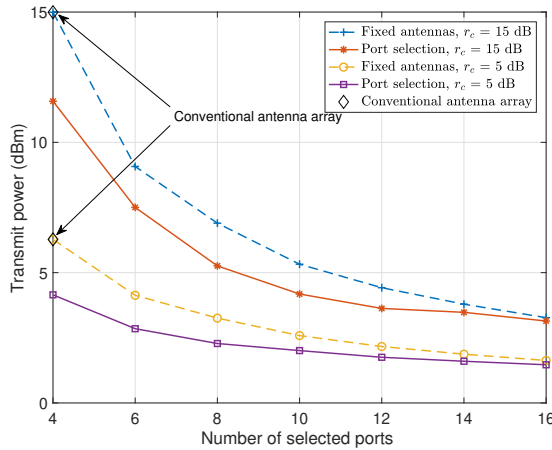


Fig. 3. Transmit power versus different number of activated ports N , compared with the baseline methods, with $r_s = 5$ dB.

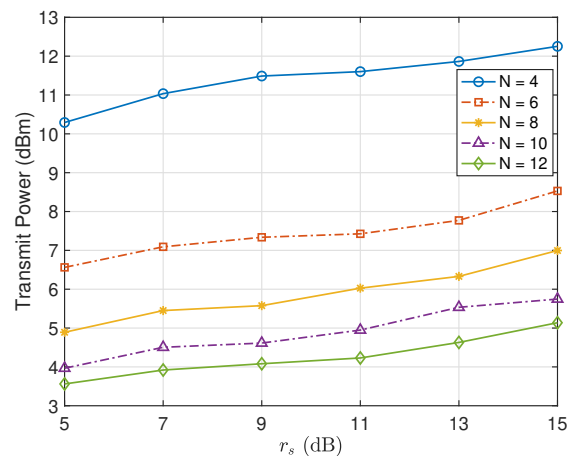


Fig. 5. Transmit power versus different sensing SNR thresholds r_s , under different number of selected ports N . The communication SNR threshold is set to $r_c = 14$ dB.

leading to an increase in the transmit power. Moreover, the results show that the algorithm enjoys a fast convergence rate, with the objective function converging within 8 iterations on both scenarios. Fig. 2 also depict the performance gaps compared with the baseline (fixed antennas) and the optimal solution. Due to the non-convexity of the problem, we conduct exhaustive search to get the optimal solution. It can be seen that the transmit power of the proposed method is only 4% higher than that what it would be required for the optimal solution when $r_c = 5$ dB, highlighting the efficiency of our approach.

In Fig 3, we provide results to numerically evaluate the effectiveness of the proposed port selection algorithm for FAS-ISAC. Firstly, compared with the conventional antenna array where only 4 ports can be implemented within the limited space, FAS achieves 33% power reduction even with 4 selected ports when $r_c = 5$ dB. When the number of activated ports of FAS increases, it can be observed that the transmit power significantly decreases. This is because of the fact that utilizing a higher number of ports provides additional DoF (i.e., spatial diversity gain), thereby achieving a higher integration gain at a

certain port. To further show the performance gain of the port selection, we compare the proposed port selection method with the fixed antennas. The fixed antenna method also minimizes the transmit power with the same constraints as the proposed port selection method, but the antennas are fixed and uniformly distributed. In Fig. 3, we can observe a noticeable drop in the transmit power of the proposed port selection method, as the spatial diversity gain is further enhanced due to the flexibility of the port position, leading to a decrease in the required transmit power to meet the S&C requirements.

Next, Fig. 4 demonstrates the transmit power results against different communication SNR requirements. As expected, the transmit power increases with the increasing communication SNR requirements in all cases of different available ports. It is worth noting that when the antenna number increases from 4 to 10, only less than half of the transmit power is required to meet the preset SNR thresholds. This indicates the potential of the fluid antenna in power saving as it is capable of providing more available ports within a limited space.

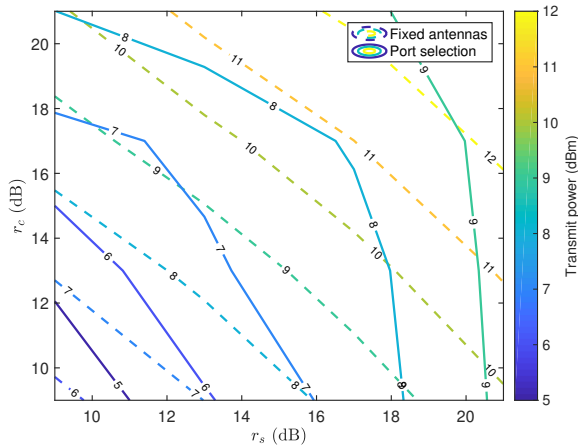


Fig. 6. S&C trade-off in the considered FAS-ISAC system with $N = 8$. The achieved minimum transmit power is labeled on the contour curve.

We further demonstrate the transmit power versus different sensing SNR thresholds in Fig. 5. Similar to the trend in Fig. 4, the transmit power is significantly decreased when more ports are activated. Although higher transmit power is required to meet a higher sensing SNR threshold, the increase in power for a larger number of activated ports, e.g., $N = 12$, is considerably smaller than that for fewer activated ports, e.g., $N = 4$. This observation suggests the effectiveness of FAS in enhancing sensing capabilities by providing an additional spatial DoF, as the FAS supports a greater number of antennas than conventional antennas within a given array size.

To investigate the trade-off between S&C, we adjust the threshold of communication SNR and sensing SNR, i.e., r_c and r_s , and solve a sequence of problems as outlined in (7b). We here present the contour curves of the achieved minimum transmit power under varying values of r_c and r_s , as shown in Fig. 6. This figure also reveals the S&C tradeoff of the proposed FAS-ISAC system. Under the same S&C constraints, the transmit power of FAS-ISAC is much lower than that of the baseline method with fixed antennas, demonstrating a better trade-off between S&C. These results indicate a significant potential for shifting the ISAC trade-off and increasing the performance bound via the implementation of FAS.

V. CONCLUSION

In this letter, we studied the model of FAS-enabled ISAC, based on which we proposed an iterative joint port selection and beamforming design. In particular, we considered a FAS-aided BS for ISAC, simultaneously performing multicast communication and target sensing. Our objective was to design a sparse beamforming vector of minimum power that meets both the communication SNR for users and the sensing SNR for target sensing. Finally, its superior performance was confirmed by the simulation results, showing that our proposed method can achieve much better performance than both the conventional antenna and uniformly distributed antennas. The potential of shifting the ISAC trade-off with FAS was verified, demonstrating the efficiency of FAS in fostering S&C performance. There are areas worth investigating in the future. For

instance, one can generalize the model and design to the case with a 2D FAS at the BS, which should offer additional DoFs and bring even more performance gain for ISAC.

REFERENCES

- [1] F. Liu *et al.*, "Integrated sensing and communications: Towards dual-functional wireless networks for 6G and beyond," *IEEE J. Sel. Areas Commun.*, vol. 40, no. 6, pp. 1728–1767, Mar. 2022.
- [2] F. Liu, Y.-F. Liu, A. Li, C. Masouros, and Y. C. Eldar, "Cramér-Rao bound optimization for joint radar-communication beamforming," *IEEE Trans. Signal Process.*, vol. 70, pp. 240–253, Dec. 2021.
- [3] J. Zou *et al.*, "Energy-efficient beamforming design for integrated sensing and communications systems," *IEEE Trans. Commun.*, vol. 72, no. 6, pp. 3766–3782, Jun. 2024.
- [4] K.-K. Wong, K.-F. Tong, Y. Shen, Y. Chen, and Y. Zhang, "Bruce Lee-inspired fluid antenna system: Six research topics and the potentials for 6G," *Front. Commun. and Net.*, no. 3, pp. 1–31, Mar. 2022.
- [5] K. K. Wong, A. Shojaefard, K. F. Tong, and Y. Zhang, "Fluid antenna systems," *IEEE Trans. Wireless Commun.*, vol. 20, no. 3, pp. 1950–1962, Mar. 2021.
- [6] H. Xu *et al.*, "Capacity maximization for FAS-assisted multiple access channels," *arXiv preprint, arXiv:2311.11037*, 2023.
- [7] K. K. Wong, A. Shojaefard, K.-F. Tong, and Y. Zhang, "Performance limits of fluid antenna systems," *IEEE Commun. Lett.*, vol. 24, no. 11, pp. 2469–2472, Nov. 2020.
- [8] K.-K. Wong and K.-F. Tong, "Fluid antenna multiple access," *IEEE Trans. Wireless Commun.*, vol. 21, no. 7, pp. 4801–4815, Dec. 2021.
- [9] K.-K. Wong, D. Morales-Jimenez, K.-F. Tong, and C.-B. Chae, "Slow fluid antenna multiple access," *IEEE Trans. Commun.*, vol. 71, no. 5, pp. 2831–2846, May 2023.
- [10] H. Xu *et al.*, "Revisiting outage probability analysis for two-user fluid antenna multiple access system," *IEEE Trans. Wireless Commun.*, vol. 23, no. 8, pp. 9534–9548, Aug. 2024.
- [11] H. Xu *et al.*, "Channel estimation for FAS-assisted multiuser mmWave systems," *IEEE Commun. Lett.*, vol. 28, no. 3, pp. 632–636, Mar. 2024.
- [12] Z. Chai, K.-K. Wong, K.-F. Tong, Y. Chen, and Y. Zhang, "Port selection for fluid antenna systems," *IEEE Commun. Lett.*, vol. 26, no. 5, pp. 1180–1184, Feb. 2022.
- [13] J. Zou, S. Sun, and C. Wang, "Online learning-induced port selection for fluid antenna in dynamic channel environment," *IEEE Wireless Commun. Lett.*, vol. 13, no. 2, pp. 313–317, Feb. 2024.
- [14] I. Valiulahi, C. Masouros, A. Salem, and F. Liu, "Antenna selection for energy-efficient dual-functional radar-communication systems," *IEEE Wireless Commun. Lett.*, vol. 11, no. 4, pp. 741–745, Apr. 2022.
- [15] K. Meng, C. Masouros, K.-K. Wong, A. P. Petropulu, and L. Hanzo, "Integrated sensing and communication meets smart propagation engineering: Opportunities and challenges," *arXiv preprint, arXiv:2402.18683*, 2024.
- [16] C. Wang *et al.*, "Fluid antenna system liberating multiuser MIMO for ISAC via deep reinforcement learning," *IEEE Trans. Wireless Commun.*, early access, DOI:10.1109/TWC.2024.3376800, Mar. 2024.
- [17] W. K. New, K.-K. Wong, H. Xu, K.-F. Tong, and C.-B. Chae, "An information-theoretic characterization of MIMO-FAS: Optimization, diversity-multiplexing tradeoff and q -outage capacity," *IEEE Trans. Wireless Commun.*, vol. 23, no. 6, pp. 5541–5556, Jun. 2024.
- [18] Z. Zhang, X. Chai, K. Long, A. V. Vasilakos, and L. Hanzo, "Full duplex techniques for 5G networks: self-interference cancellation, protocol design, and relay selection," *IEEE Commun. Mag.*, vol. 53, no. 5, pp. 128–137, May 2015.
- [19] O. Mehanna, N. D. Sidiropoulos, and G. B. Giannakis, "Multicast beamforming with antenna selection," in *Proc. IEEE Int. Wksp. Signal Process. Adv. Wireless Commun. (SPAWC)*, 17–20 Jun. 2012, Cesme, Turkey.
- [20] M. Razaviyayn, M. Sanjabi, and Z.-Q. Luo, "A stochastic successive minimization method for nonsmooth nonconvex optimization with applications to transceiver design in wireless communication networks," *Springer*, vol. 157, pp. 515–545, 2016.
- [21] C. E., W. M., and B. S., "Enhancing sparsity by reweighted l_1 minimization," *J. Fourier Analysis and Applications*, vol. 14, no. 5, pp. 877–905, Dec. 2008.